TISSUE ENGINEERING: Part C
Volume 20, Number 11, 2014

DOI: 10.1089/ten.tec.2013.0411

Enhanced Differentiation of Human Embryonic Stem Cells on Extracellular Matrix-Containing Osteomimetic Scaffolds for Bone Tissue Engineering

Katy Rutledge,[1] Qingsu Cheng,[2] Marina Pryzhkova, PhD,[1] Greg M. Harris,[1] and Ehsan Jabbarzadeh, PhD[1–3]

Current methods of treating critical size bone defects include autografts and allografts, however, both present major limitations including donor-site morbidity, risk of disease transmission, and immune rejection. Tissue engineering provides a promising alternative to circumvent these shortcomings through the use of autologous cells, three-dimensional scaffolds, and growth factors. We investigated the development of a scaffold with native bone extracellular matrix (ECM) components for directing the osteogenic differentiation of human embryonic stem cells (hESCs). Toward this goal, a microsphere-sintering technique was used to fabricate poly(lactic-*co*-glycolic acid) (PLGA) scaffolds with optimum mechanical and structural properties. Human osteoblasts (hOBs) were seeded on these scaffolds to deposit bone ECM for 14 days. This was followed by a decellularization step leaving the mineralized matrix intact. Characterization of the decellularized PLGA scaffolds confirmed the deposition of calcium, collagen II, and alkaline phosphatase by osteoblasts. hESCs were seeded on the osteomimetic substrates in the presence of osteogenic growth medium, and osteogenicity was determined according to calcium content, osteocalcin expression, and bone marker gene regulation. Cell proliferation studies showed a constant increase in number for hESCs seeded on both PLGA and ECM-coated PLGA scaffolds. Calcium deposition by hESCs was significantly higher on the osteomimetic scaffolds compared with the control groups. Consistently, immunofluorescence staining demonstrated an increased expression of osteocalcin in hESCs seeded on ECM-coated osteomimetic PLGA scaffolds. Gene expression analysis of RUNX2 and osteocalcin further confirmed osteogenic differentiation of hESCs at the highest expression level on osteomimetic PLGA. These results together demonstrate the potential of PLGA scaffolds with native bone ECM components to direct osteogenic differentiation of hESCs and induce bone formation.

Introduction

LIKE MANY TISSUES in the body, bone has a natural ability to repair minor injuries resulting from disease or small fractures. Despite this, it is estimated that over 800,000 bone graft procedures are completed yearly in the United States to facilitate repair from large-scale trauma.[1–3] Current treatment methods for critical-sized defects (CSDs) include (i) autografts, where the patient's own bone tissue is removed from one area and placed in the site of deficiency, (ii) allografts, where bone from a cadaver is used to replace the damaged tissue, (iii) and synthetic grafts, where manufactured materials are implanted and used to treat the CSD.[4–6] Autografts are considered the gold standard in clinical applications because of their osteoconductivity, osteoinductivity, and osteogenecity, however, a secondary surgery is required for implementation. There is also a risk of disease transfer, rejection by the host, and large bone defects cannot be treated by autografts.[3,7–11] Long-term storage of bone tissue for allografts causes bone architecture to dramatically weaken and most of the osteoprogenitor cells are no longer viable. Synthetic grafts cannot fully incorporate with the host tissue and are susceptible to fatigue, fracture, and wear.[12] Therefore, there is a need for better treatment options for patients with CSDs.

Tissue engineering presents a new avenue for developing bone grafts by combining the use of cells, specific signaling molecules, and three-dimensional (3D) substrates.[13–16] Recent efforts toward developing bone graft substitutes focus on 3D scaffold design. The 3D matrix should mimic the structure of bone, in which porosity and mechanical strength are important characteristics. A scaffold should also guide the integration of host cells, the differentiation of transplanted cells, and promote bone extracellular matrix (ECM) formation on the surface of the substrate.[17] In this spirit, biodegradable scaffolds

[1]Department of Chemical Engineering, University of South Carolina, Columbia, South Carolina.
[2]Biomedical Engineering Program, University of South Carolina, Columbia, South Carolina.
[3]Department of Orthopedic Surgery, University of South Carolina School of Medicine, Columbia, South Carolina.

provide a temporary matrix for cells to attach, proliferate, and deposit ECM.[18–22] Polymers such as poly(lactic acid), poly(glycolic acid), and their copolymers poly(lactic-*co*-glycolic acid) (PLGA) have demonstrated success in bone tissue engineering applications due to their biocompatibility, osteoconductivity, and mechanical properties.[23–27]

Cells seeded on scaffolds may stimulate signaling events that trigger host cells to migrate and integrate with the newly formed tissue, thus accelerating wound healing process following scaffold implantation. Both human mesenchymal stem cells (hMSCs) and human embryonic stem cells (hESCs) have been investigated as a source of new bone tissue for grafts. hESCs possess the unique ability to self-renew and have the potential to differentiate into any cell type formed from the three germ layers.[28,29] hESCs offer a promising tool for biomedical research as they can be used in developmental studies, disease modeling, drug testing, and regenerative medicine.[30] These stem cells are derived from the inner cell mass of a preimplantation embryo during the blastocyst stage.[31–33] The maintenance and culture of hESCs usually involves growing cells in feeder-dependent or feeder-free conditions, and cells are kept in colonies to preserve an undifferentiated state. Embryoid bodies (EBs) are commonly used to mimic the three-dimensionality of development during gastrulation and the formation of the three germ layers *in vivo*.[34] The limitation of employing EBs for differentiation studies arises from the fact that the yield of desired cells is much lower than the initial amount of cells.[35] To use hESCs for differentiation experiments, cells must retain pluripotency and self-renewal capabilities, and it is imperative to parse the underlying developmental mechanisms involved in osteogenesis to successfully engineer bone tissue.

Numerous studies have demonstrated the potential of hMSCs in bone tissue engineering applications.[36–41] While they eliminate the controversy surrounding hESCs, they also present key disadvantages such as the loss of proliferation capabilities with increasing passages and their infrequency in the stroma indicates a limited population of cells that can actually differentiate into osteogenic lineage.[42,43] Studies conducted in animal models demonstrated that the amount of bone formed from hMSCs was insufficient to bridge a large bone defect.[44] Furthermore, clinical trials have also determined hMSCs inadequate for repairing CSDs due to lack of cell number and requirement of additional osteoinductive signals.[45] Another shortcoming with using hMSCs for tissue engineering studies is that multipotency limits their differentiation potential to specific cell types.[46,47] Since the formation of bone requires numerous varieties of cells,[48] hMSCs are not an ideal cell source.

hESCs are promising candidates for bone tissue engineering applications since they can differentiate into every cell type found in bone.[49–54] Osteoblasts, osteoclasts, nerve cells, and vascular cells all contribute to bone architecture and function, and given the correct signals, hESCs will become these cell types.[48] hESCs are the superior choice for bone tissue regeneration strategies, but they offer obstacles to overcome as well. hESCs are difficult to culture and scaffold surface modification is required for cell attachment; substrates traditionally have been coated with protein cocktails such as Matrigel or Geltrex to promote cell adhesion. Bone-forming osteoblast cells or osteoprogenitor cells can also be used to deposit natural ECM proteins onto the substrate for hESC attachment. To date, great strides have been taken in using native bone components to create scaffolds to promote the growth of osteoblast-like cells, however, most approaches focus on one element of the ECM as opposed to the entire network.[55–64] Decellularized scaffolds composed of the organic and inorganic elements of bone ECM are osteoinductive and osteoconductive. The interactions between cells and the ECM have the ability to define cell development and function.[65] By using osteoblasts to deposit ECM, a natural bone microenvironment is created that will stimulate hESCs to differentiate into osteogenic lineage. Although numerous studies have shown the potential of decellularized scaffolds, there is a lack of characterization of the signals involved in using natural ECM to direct the differentiation of hESCs and there is a need for determining which spatial and temporal cues control the diverse development of bone.

In this study, we developed an osteomimetic PLGA scaffold that will allow hESC attachment, proliferation, and differentiation into osteogenic lineage. We hypothesized that the native bone ECM deposited by hOBs will cover the surface of the microsphere-sintered PLGA scaffolds, and will direct the differentiation of hESCs into bone lineage by providing a natural bone tissue microenvironment. This hypothesis is based on studies demonstrating the use of native bone ECM components in stimulating hESCs and hMSCs to differentiate into osteoblasts.[55,56] To this end, the properties of the osteomimetic scaffolds such as ECM composition and morphology and the *in vitro* differentiation of hESCs into bone tissue were investigated.

Materials and Methods

Synthesis of PLGA microsphere sintered scaffolds

Scaffolds with diameters of 10 mm and heights of 2 mm were fabricated and used in this study. Briefly, PLGA (75:25 lactide to glycolide ratio; Lactel Absorbable Polymers) was dissolved in dichloromethane (Sigma) to form a 1:4 w/v polymer solution. This solution was added to a 1% poly(vinyl alcohol) solution (Sigma) while being stirred at 330 rpm for 24 h to allow adequate evaporation of the solvent. After harvesting the microspheres by vacuum filtration, the samples were washed with deionized (DI) water and stored at −20°C for 24 h. The microspheres were lyophilized to completely remove all moisture. Commercially available micron sieves were used to isolate microspheres of diameter 500–700 μm and they were placed into stainless steel molds, heated at 85°C for 12 h, and sintered into cylindrical disks.

hOB cell culture and PLGA scaffold seeding

P3 human osteoblasts hFOB 1.19 (ATCC) were cultured in osteogenic differentiation medium consisting of DMEM/F12 (Gibco), 10% fetal bovine serum (FBS; Atlas), 10 mM β-glycerophosphate (Sigma), 50 μg/mL ascorbic acid (Sigma), 1 μM dexamethasone (Sigma), and 1% penicillin/streptomycin (Invitrogen). Medium was changed every other day and cells were passaged once 80% confluency was reached. After two passages, human osteoblasts (hOBs) were trypsinized and seeded on the scaffolds.

Before seeding hOBs on the PLGA substrates, scaffolds were sterilized by immersion in 70% ethanol for 10 min,

washed 3× with phosphate buffered saline (PBS), and exposed to UV light for 30 min on each side. hOBs were detached from the culture flask using trypsin and 20 μL (containing 5×10^5 cells) of cell suspension were seeded per scaffold. Cells were cultured in osteogenic medium for 14 days and culture medium was changed every other day.

Cell attachment and proliferation was analyzed during the 14 day culture period using 3-(4,5-dimethylthiazol-2-yl)-5-(3-carboxymethoxyphenyl)-2-(4-sulfophenyl)-2H-tetrazolium (MTS; Promega) colorimetric assay. Three hundred microliters of fresh media was added to each scaffold, and incubated for 2 h with 60 μL of MTS solution. The resulting solution was diluted 1:5 and the absorbance was read at 492 nm using a UV Vis Spectrophotometer.

Decellularization and analysis

PLGA scaffolds were decellularized by adding a sterile solution of 0.25% Triton X-100 (Sigma) and 0.25% deoxycholate (Alfa Aesar) dissolved in PBS for 30 min at 4°C, followed by incubation at 37°C for several hours. The decellularization solution was removed and scaffolds were washed 3× with PBS.

Decellularized scaffolds were characterized by Alizarin Red S staining, calcium quantification, alkaline phosphatase (ALP) staining, collagen II staining, and scanning electron microscopy (SEM). To visualize the mineralized ECM, samples were first fixed in 10% formalin for 30 min and washed 3× with DI water. Alizarin Red S staining solution (pH 4.2–4.5; Alfa Aesar) was added to the samples at a concentration of 0.02 mg/mL and incubated for 5 min. Samples were washed for 5 h in 100% ethanol and ethanol was changed every 30 min. Mineralized ECM was visualized with a Zeiss light microscope. To quantify the mineralized calcium, the O cresolphthalein complexone (Sigma) method was used. DI water was used to wash the scaffolds 3×, and 0.6 M hydrochloric acid was employed to homogenize the samples followed by 4 h of shaking at 4°C for calcium extraction. The amount of calcium was determined by reading the absorbance at 570 nm with a UV Vis spectrophotometer. ALP was detected by using ALP kit #85 (Sigma) in which scaffolds were fixed with 10% formalin for 30 min and washed 3× with PBS. The Fast Blue capsule was dissolved in napthanol to prepare the staining solution, added to the scaffold, and incubated for 30 min. The scaffolds were washed 3× with PBS followed by incubation in the Mayer's hematoxylin solution for 10 min. ALP was observed and photographed using a Nikon E600 light microscope. To determine collagen II expression, scaffolds were fixed in 10% formalin for 30 min and washed 3× with PBS. After washing, scaffolds were permeabilized using 0.1% Triton X-100 solution for 15 min. Cells were washed 3× with PBS and blocked using 1% bovine serum albumin (Sigma) in PBS for 30 min. FITC-conjugated anti-collagen II antibody (1:100; Thermo) was added to the scaffolds for 1 h followed by washing 3× with PBS. Cell nuclei were stained by adding 4′-6-diamidino-2-phenylindole (DAPI, 1:25; Sigma) antifade to the decellularized constructs. The samples were visualized using a Zeiss 510 LSM confocal microscope and a water immersion lens. For SEM analysis, cells on the scaffolds were fixed in 1% glutaraldehyde for 1 h followed by fixation in 3% glutaraldehyde at 4°C overnight. The scaffolds were dehydrated sequentially by a series of increasing ethanol concentrations (10%, 30%, 50%, 70%, 90%, 95%, 95%, 100%, and 100%) for 15 min each. PGLA scaffolds were dried overnight and coated with gold/palladium. Scaffolds were observed under Zeiss Ultra Plus FESEM after coating.

hESC seeding

hESCs from cell line h9 (Wicell) p38 were grown on a feeder layer of mitomycin C inactivated mouse embryonic fibroblasts (MEF) (cell line PMEF-CFL; Millipore) in medium consisting of DMEM/F12 (Gibco), 20% Knock-out serum replacement (Gibco), 3.5 mM L-Glutamine (Invitrogen), 100 μM β-mercaptoethanol (Sigma), 1% nonessential amino acids (Invitrogen), and 10 ng/mL bFGF (Peprotech). The MEF cells were used as a feeder layer and cultured in high glucose with L-glutamine DMEM (Gibco) supplemented with 10% FBS and 1% penicillin/streptomycin (Invitrogen). Mitomycin C (10 mg/mL; Sigma) was used to inactivate MEF cells for 2.5 h, after which cells were seeded at a density of 2.1×10^4 cells/cm^2 on tissue culture plastic coated with 1% gelatin (Sigma). Cells were cultured for 1 day in MEF media prior to hESC seeding. hESCs were detached from the tissue culture plate by a combination of the enzyme collagenase IV (Sigma) and by manually scraping. Approximately 50,000 hESCs were seeded per scaffold, and MEF-conditioned hESC medium was used to ensure cell attachment overnight. The following day, culture medium was changed from conditioned medium to osteogenic differentiation medium. Osteogenic differentiation medium was changed the following day to remove cell debris, then every 3 days for the remainder of the experiment.

For the control groups, two-dimensional (2D) tissue culture polystyrene (TCPS) and Geltrex-coated PLGA scaffolds were used. To coat the PLGA scaffolds and 2D culture plates, 2.5 μL of Geltrex (Invitrogen) was mixed with 1 mL of cold DMEM/F12, added to the scaffolds and plates, and incubated at 37°C for 1 h, then incubated at room temperature for 1 h. Approximately 50,000 hESCs were seeded per well of a 24-well plate, and per Geltrex-coated PLGA scaffold.

Cell attachment, growth, and morphology

At predetermined time points, cell morphology was assessed using SEM. Cells on the scaffolds were prepared as previously described and observed under a Zeiss Ultra Plus FESEM after coating.

Cell proliferation on scaffolds was assessed using MTS (Promega) colorimetric assay. Three hundred microliters of fresh media was added to each scaffold, and incubated for 2 h with 60 μL of MTS solution. The resulting solution was diluted 1:5 and the absorbance was read at 492 nm using a UV Vis Spectrophotometer.

Cytoskeleton formation was observed by F-actin staining. Cells on the scaffolds were fixed at room temperature in 10% formalin for 30 min. After washing scaffolds 3× with PBS, cells were permeabilized using a 0.1% Triton X-100 solution for 15 min. Cells were then washed 3× with PBS and blocked using 4% Goat Serum in PBS for 30 min. TRITC-conjugated phalloidin (1:40; Invitrogen) was added to the scaffolds for 1 h, samples were washed 3× with PBS, and cell nuclei were stained with DAPI (1:25; Sigma).

Stained cells were visualized using a Zeiss 510 LSM confocal microscope under a water immersion lens.

Assessment of osteogenic differentiation

Osteogenic differentiation was assessed by monitoring the calcium deposition, osteocalcin expression, and quantitative real-time polymerase chain reaction (qRT-PCR) analysis of RUNX2 and BGLAP genes.

Calcium was quantified using the O cresolphthalein complexone (Sigma) method. At predetermined time points, cell culture medium was removed from the scaffolds and cells were washed 3× with DI water. 0.6 M hydrochloric acid was used to homogenize the samples followed by 4 h of shaking at 4°C for calcium extraction. Samples were compared against $CaCl_2$ standards and the amount of calcium was determined by reading the absorbance at 570 nm with a UV Vis spectrophotometer.

ECM mineralization was assessed using Alizarin Red S staining. Samples were fixed in 10% formalin for 30 min and washed 3× with DI water. Alizarin Red S staining solution (pH 4.2–4.5; Alfa Aesar) was added to the samples at a concentration of 0.02 mg/mL and incubated for 5 min. Samples were washed for 5 h in 100% ethanol, and ethanol was changed every 30 min. Mineralized ECM was visualized with a Nikon E600 light microscope.

Osteocalcin was qualitatively observed by immunofluorescence staining. In brief, cells were fixed in 10% formalin for 30 min, followed by washing 2× with a rinse buffer (20 mM Tris-HCL and 0.05% Tween-20 in PBS; Sigma). The sample was then permeabilized with 0.1% Triton X-100 (Sigma) in PBS for 15 min, and washed 2× with the rinse buffer. Cells were blocked with 4% goat serum in PBS for 30 min. The primary antibody, osteocalcin (1:50; R&D Systems), was added to the scaffolds and incubated for 60 min. Following the primary antibody incubation, the samples were washed 3× with the rinse buffer for 5 min each time. Then, Alexafluor 594 (1:1000; Invitrogen) was added to the samples and incubated for 1 h, followed by DAPI (1:25; Sigma) nuclear stain. Stained cells were visualized using a Zeiss 510 LSM confocal microscope under a water immersion lens.

Total RNA was extracted from the samples using the GeneJET RNA Purification Kit (Thermo Scientific). One microgram of RNA was used as a template for single-strand cDNA synthesis with the RevertAid First Strand cDNA Synthesis Kit (Thermo Scientific). In brief, RNA was prepared by first removing genomic DNA from the sample. The reaction buffer with $MgCl_2$, DNase, I., and nuclease-free water was added to 1 μg of RNA to a total volume of 10 μL. The sample was incubated at 37°C for 30 min, then 1 μL 50 mM EDTA was added and incubated at 65°C for 10 min. The template RNA was mixed with 1 μL oligo $(dT)_{18}$ primer and nuclease-free water to a volume of 12 μL, followed by the addition of 4 μL of 5× Reaction Buffer, 1 μL Ribolock RNase Inhibitor, 2 μL 10 mM dNTP Mix, and 1 μL RevertAid M-MuLV Reverse Transcriptase. This mixture was then incubated at 42°C for 1 h. The SensiFAST SYBR No-ROX Kit (Bioline) was used for qRT-PCR. One hundred nanograms of cDNA was mixed with 10 μL 2× SensiFAST SYBR No-ROX Mix, 10 μM forward primer, 10 μM reverse primer, (see Table 1 for sequences), and nuclease-free water to 20 μL. A three-step cycling was used on a Bio-Rad CFX96 instrument: 1 cycle of 95°C for 2 min to activate the polymerase, followed by 40 cycles of 95°C for 5 s to denature, 65°C for 10 s for annealing, then 10 s at 72°C for extension. Gene expression of RUNX2 and BGLAP were normalized to GAPDH and presented as relative values.

Table 1. Primers Used for Quantitative Real-Time Polymerase Chain Reaction

Primer name	*Sequence*
RUNX2 forward	5′-CTC ACT ACC ACA CCT ACC TG-3′
RUNX2 reverse	5′-TCA ATA TGG TCG CCA AAC AGA TTC-3′
BGLAP forward	5′-GGC GCT ACC TGT ATC AAT GG-3′
BGLAP reverse	5′-TCA GCC AAC TCG TCA CAG TC-3′

Statistical analysis

Three samples ($n = 3$) were analyzed per condition unless otherwise stated. Error bars in graphs represent mean ± standard deviation. One-way analysis of variance was used to determine statistical significance. Comparison between the two means was determined by the Tukey test and statistical significance was defined as $p \leq 0.05$.

Results

Figure 1 demonstrates the growth of hOBs on PLGA scaffolds during the 14 day culture period. The number of cells was determined for days 1, 4, 7, and 14. Cells attached to the scaffolds and cell number steadily increased at each sequential time point. From this assay it was confirmed that cells were proliferating, therefore depositing ECM on the substrate.

Figure 2 shows characterization of the microsphere-sintered PLGA scaffolds. The scaffolds were all highly porous with interconnected structures, and demonstrated similar architecture to that of trabecular bone. SEM images

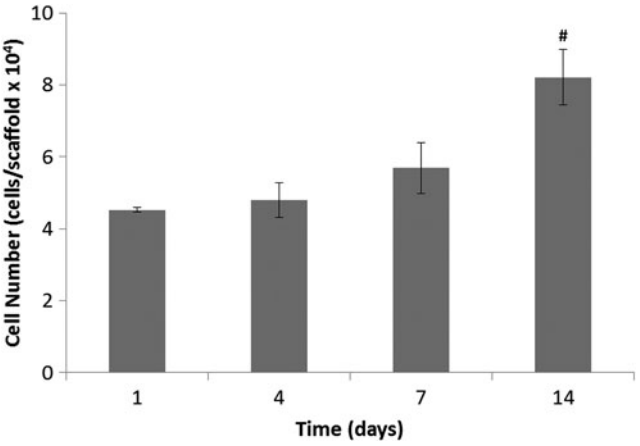

FIG. 1. Proliferation of hOBs on PLGA scaffolds at time points of days 1, 4, 7, and 14. Cell number steadily increased during the 14-day culture period. # represents a significant difference in cell number between days 14 and 1 at a significance level of $p < 0.2$. hOBs, human osteoblasts; PLGA, poly(lactic-*co*-glycolic acid).

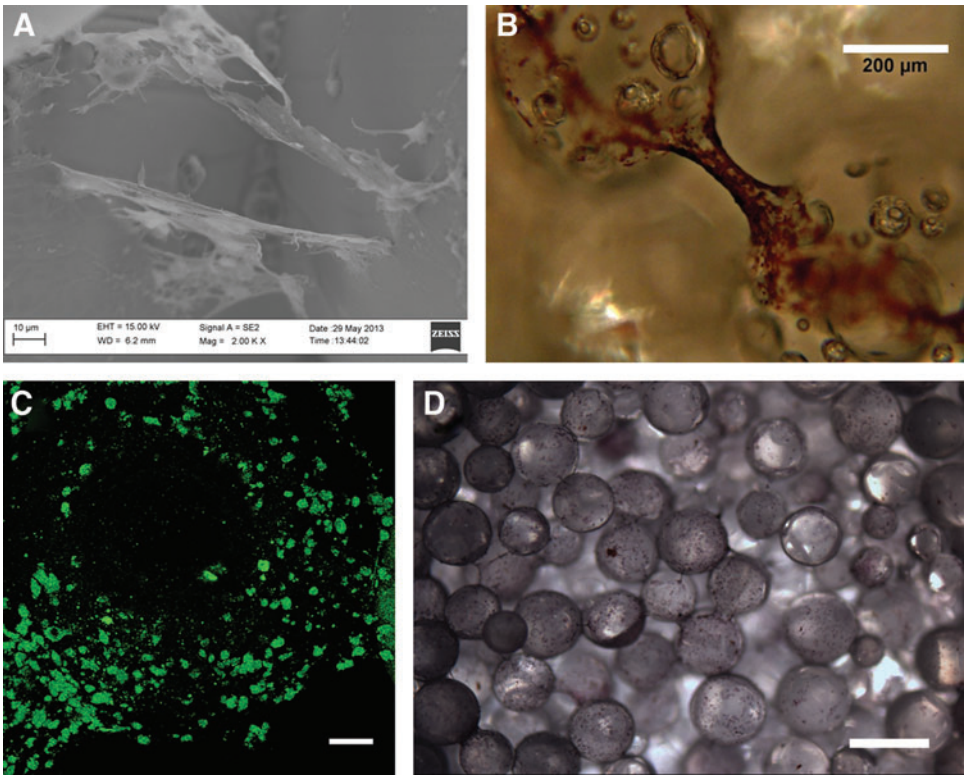

FIG. 2. Analysis of osteomimetic scaffolds. **(A)** SEM image of ECM covering surface of PLGA scaffold, scale bar 10 μm and magnification 2000×; **(B)** Alizarin Red S staining of calcium deposited by hOBs on scaffold surface, scale bar 200 μm and magnification 10×; **(C)** Collagen II staining of ECM confirms ECM composition, scale bar 50 μm and magnification 20×; **(D)** ALP staining of ECM covering surface of PLGA scaffold, scale bar 500 μm and magnification 4×. ALP, alkaline phosphatase; ECM, extracellular matrix; SEM, scanning electron microscopy. Color images available online at www.liebertpub.com/tec

of decellularized scaffolds (Fig. 2A) showed ECM deposition covering the surface of the microspheres, with collagen fibrils clearly defined. Alizarin Red S staining indicated the presence of calcium in the mineralized ECM (Fig. 2B), while collagen II staining demonstrated the presence of collagen II in the ECM (Fig. 2C). The enzyme ALP was also found on the surface of the decellularized PLGA scaffolds, as shown by the purple/blue stain indicative of ALP (Fig. 2D). The quantification of the mineralized calcium on the decellularized scaffolds indicated that an average of 1.17 μg of calcium was present per construct.

Figure 3 demonstrates cell attachment and morphology of hESCs (Fig. 3A), and proliferation and morphology of hESC-derived osteogenic progenitors (Fig. 3B). The hESC colonies were able to attach to the decellularized matrix, initially in large, compact colonies (Fig. 3A). They continued to grow

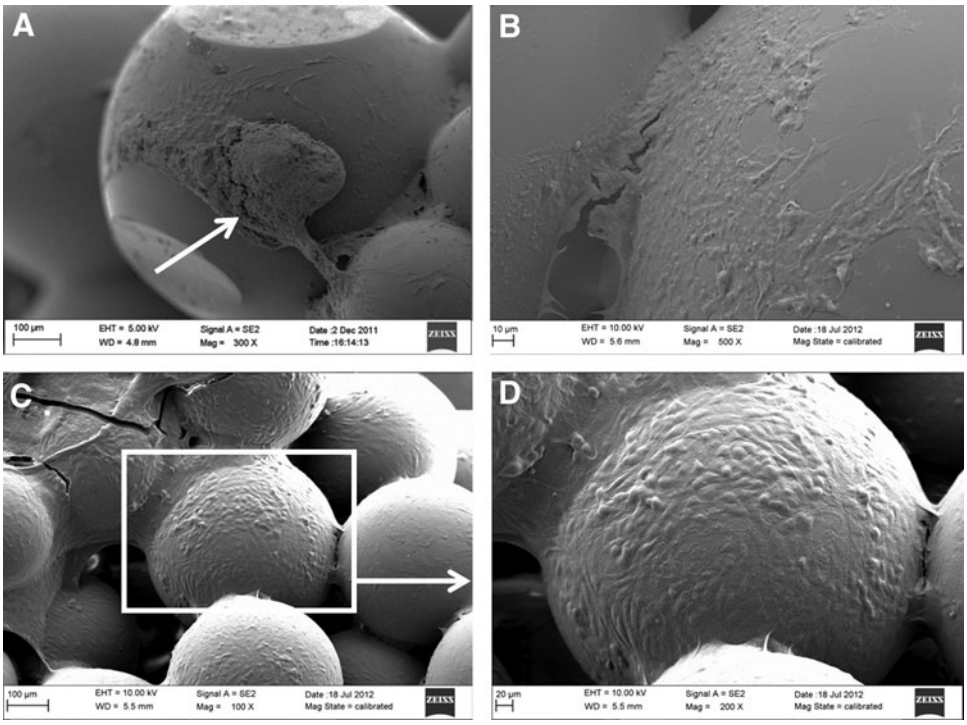

FIG. 3. SEM images of hESCs and hESC-derived osteogenic progenitors on osteomimetic scaffolds. **(A)** Day 0 shows colony attachment, indicated by white arrow, scale bar 100 μm and magnification 300×; **(B)** Day 7 demonstrates the onset of differentiation, scale bar 10 μm and magnification 500×; **(C)** Day 35 shows differentiated cells with osteoblast-like morphology, scale bar 100 μm and magnification 100×; **(D)** Day 35 differentiated hESCs, scale bar 20 μm and magnification 200×. hESCs, human embryonic stem cells.

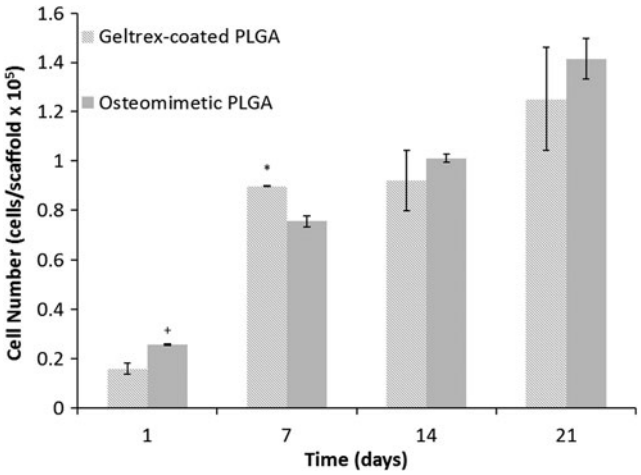

FIG. 4. Proliferation of hESCs on Geltrex-coated PLGA and osteomimetic scaffolds, shown as cell number/scaffold. * and + represent significant difference in cell number between the Geltrex-coated PLGA and the osteomimetic scaffolds at significance levels of $p < 0.05$ and 0.1, respectively.

and spread, and after 7 days the cells no longer exhibited an undifferentiated hESC phenotype (Fig. 3B). The cells formed bridges between microspheres and fully covered the scaffold surface at day 35 (Fig. 3C, D). Cell proliferation was monitored by the MTS assay, and in all conditions, cells increased in number (Fig. 4). Interestingly, the decellularized scaffold group had the highest cell numbers compared with the Geltrex-coated PLGA group, with the exception of day 7. Cytoskeleton organization and morphology was observed by SEM and immunofluorescence staining of F-actin and DAPI (Fig. 5A, B, respectively). We observed that the cells proliferated on the surface of the scaffolds and within the pores, and there was no noticeable variation in cytoskeleton structure and morphology among the groups.

Osteogenic differentiation was assessed by observing calcium content, osteocalcin expression, and qRT-PCR to quantify osteogenic marker genes. The highest level of calcium content was expressed by the hESCs on the decellularized scaffolds, followed by the Geltrex-coated PLGA group, with the 2D TCPS group demonstrating the least amount of mineralized matrix (Fig. 6A). The immunofluorescence staining of the differentiated cells on the scaffolds showed that osteocalcin was present in the differentiated hESCs on the decellularized scaffolds, Geltrex-coated PLGA scaffolds, and 2D TCPS. The highest level of osteocalcin was detected in the decellularized scaffold, as shown in Figure 5C. To quantitatively evaluate the marker genes indicative of osteogenic differentiation, qRT-PCR was employed. It was found that the decellularized scaffolds and the PLGA scaffolds exhibited the highest expression of RUNX2 compared with the 2D culture plate (Fig. 6B). BGLAP levels were the highest in decellularized scaffolds, followed by the PLGA scaffolds and 2D TCPS (Fig. 6C).

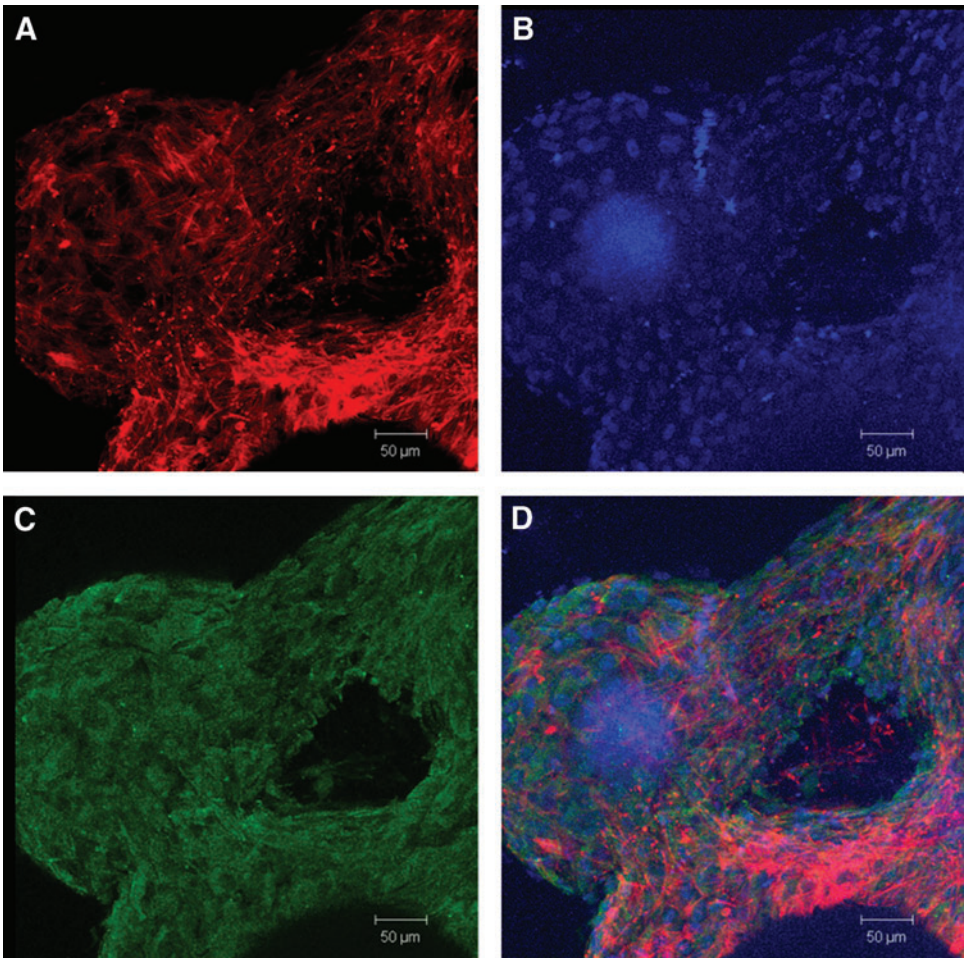

FIG. 5. Confocal images of day 35 differentiated hESCs on osteomimetic PLGA, scale bars 50 µm and magnification 20×. **(A)** Actin demonstrates cytoskeleton formation; **(B)** DAPI shows nuclear staining; **(C)** Osteocalcin expression; and **(D)** a merged image of actin, DAPI, and osteocalcin. DAPI, 4′-6-diamidino-2-phenylindole. Color images available online at www.liebertpub.com/tec

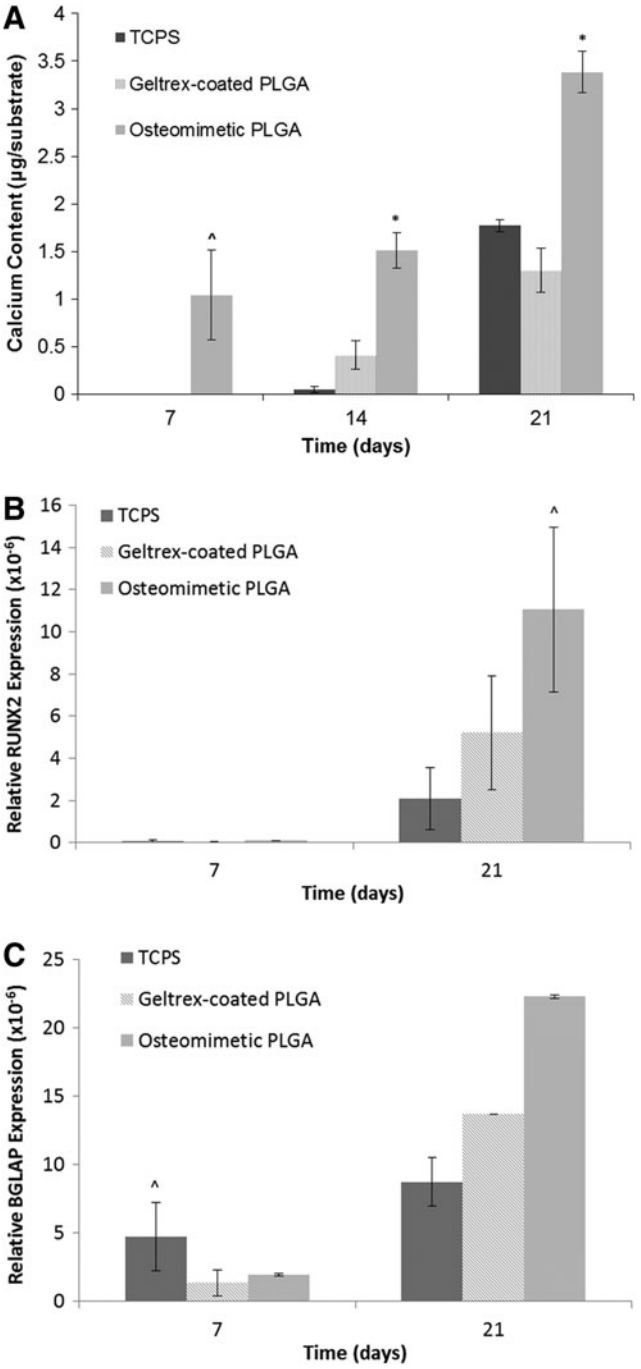

FIG. 6. Calcium deposition and gene expression of differentiated hESCs on 2D culture plates, Geltrex-coated PLGA, and osteomimetic PLGA. * and ^ represent significant difference in calcium content and gene expression by cells on osteomimetic scaffolds compared with Geltrex-coated PLGA and 2D tissue culture plates at significance levels of $p < 0.05$ and 0.5, respectively. **(A)** Calcium quantification for each group represented as microgram/substrate where the substrate is the scaffold for the osteomimetic PLGA and geltrex-coated PLGA groups, and the 2D well surface for the TCPS group; **(B)** Relative RUNX2 gene expression ($n = 2$); **(C)** Relative BGLAP gene expression ($n = 2$). All values were normalized to GAPDH. 2D, two-dimensional; TCPS, tissue culture polystyrene.

Discussion

The ability to develop a 3D porous scaffold with comparable mechanical and structural properties to that of natural bone governs the success of many bone tissue engineering endeavors. Bone is a complex tissue composed of an architectural hierarchy: (i) the macrostructure, which is made up of cortical and cancellous bone, (ii) the microstructure, which is composed of osteons, haversian systems, and trabeculae, (iii) the submicrostructure, which is comprised of the lamellae, (iv) the nanostructure, which is predominately composed of collagen I fibers, and (v) the sub-nanostructure made up of mineralized matrix, smaller collagen subunits, and other organic proteins.[66] Due to this intricate tissue configuration, recreating bone structure is a major hurdle in generating scaffolds. Another obstacle in bone tissue engineering studies is deciphering specific roles of scaffold design parameters governing *in vitro* osteogenic differentiation and *in vivo* osteointegration.

The research work described in this study centers in on designing an osteomimetic scaffold composed of microsphere-sintered PLGA scaffolds and native bone ECM components secreted by osteoblast cells. These scaffolds were then applied to an *in vitro* study that analyzed the osteogenic differentiation of hESCs seeded on these decellularized scaffolds as compared to the control Geltrex-coated PLGA scaffolds and 2D TCPS group. It was hypothesized that hESCs seeded on the native bone ECM scaffolds would exhibit faster osteogenic differentiation and greater expression of mineralized matrix, higher levels of osteocalcin expression, and greater levels of bone marker genes such as RUNX2 and osteocalcin. A rationale for this work was based on recent studies that demonstrated the potential of decellularized bone matrices in directing the differentiation of hESCs and hMSCs into osteogenic lineage.[55,56]

In this study, we used microsphere-sintering to develop scaffolds. This fabrication technique produces scaffolds of tunable porosity and mechanical strength within the range of trabecular bone.[26,67] Osteoblasts readily attach to PLGA substrates through proteins in the FBS adsorbing to the surface of scaffolds allowing for integrin–ligand interactions, however, hESCs need surface modifications to adhere to the scaffolds. To alter the surface of the substrate for promoting the attachment of hESCs, a native bone microenvironment was generated by seeding hOBs on the PLGA scaffolds, then removing the cells while leaving the ECM intact. During the 14-day culture period, hOBs proliferated on the scaffolds and deposited ECM on the surface of the substrate. The ECM secreted by the osteoblasts contained calcium, ALP, collagen II, and other proteins found in bone structure. Since bone is formed via endochondral ossification in the embryo, the collagen II structure laid down by the hOBs is thought to stimulate the natural signaling pathways for hESCs to differentiate into osteogenic lineage.[68]

Cell attachment and morphology was assessed by using SEM. Cell shape is indicative of adhesion since cells that have a spread-out morphology have more focal adhesions and greater cell-substrate contact than cells exhibiting a round morphology. Differentiated hESCs on the Geltrex-coated PLGA scaffold and decellularized PLGA scaffold demonstrated a spread phenotype, and the cells were able to migrate throughout the scaffold by forming extensions

between adjacent microspheres. This result is consistent with previous studies demonstrating the proliferation of primary fibroblasts and osteoblasts on PLGA microsphere-sintered scaffolds.[26,67,69]

In line with other studies, our *in vitro* evaluation of the decellularized scaffolds demonstrated a higher level of osteogenic differentiation compared with the control groups. hESCs underwent differentiation over a 35 day period as a result of physical cues from the native ECM scaffolds and chemical growth factors in the differentiation media. The extent of differentiation was measured by quantifying calcium expression, in addition to immunofluorescence staining of osteocalcin and by analyzing gene expression of osteocalcin and RUNX2 by qRT-PCR. Common methods of analyzing osteogenic differentiation include quantifying ALP, collagen I, noncollagenous proteins such as osteocalcin, and the existence of bone apatite[70]; however, these qualities are not unique to bone-forming osteoblasts. The most stand-alone method of determining osteoblast differentiation besides analyzing mRNA is the observation of a cell-mediated calcified ECM.[71] We determined calcium content of each experimental group, and the osteomimetic scaffolds expressed the highest amount compared with the 2D control and Geltrex-coated PLGA scaffolds. Our study showed that 3D microenvironments produced from microsphere-sintered PLGA scaffolds generates a higher level of hESC differentiation into osteogenic lineage compared with cells grown on 2D tissue culture plates. Furthermore, our results from these tests demonstrate that the presence of native bone ECM on 3D PLGA scaffolds leads to an elevated expression of osteogenic markers. RUNX2 is the main transcription factor for the osteoblast, and it is exclusively required for osteoblast differentiation.[48] RUNX2 expression determines osteogenic lineage commitment; therefore, the upregulation of RUNX2 mRNA quantified by qRT-PCR demonstrates the differentiation of hESCs into osteoblasts.

The advantage of our synthetic scaffolds coated with bone ECM is that we can design the polymer to mimic the structure of trabecular bone while exhibiting similar mechanical properties. This eliminates the risk of immunogenicity associated with using bone from humans or animals that has been decellularized. Decellularized scaffolds offer a native bone microenvironment in which stem cells can receive signals from the proteins and embedded growth factors. These signals govern cell type and function.

The enthusiasm for using hESCs as a source for bone tissue is hindered by ethical concerns and the need to establish protocols to obtain a homogenous population of differentiated cells.[28,72] Also, the risk of teratoma formation is a major issue in using hESCs *in vivo*.[73,74] Future directions of this study include delineating the mechanisms by which native bone ECM components and architecture modulates the osteogenic differentiation of hESCs. This will enable us to design a scaffold that induces cells to exclusively form components of bone and it will ensure that teratoma formation will not occur.

Conclusions

In this study, osteomimetic PLGA scaffolds were fabricated by microsphere-sintering and by utilizing hOBs to deposit bone ECM on the surface of the polymer. The native bone ECM substrates resembled bone tissue in composition. The potential of these scaffolds as bone graft substitutes was evaluated by the *in vitro* differentiation of hESCs on the osteomimetic substrates and Geltrex-coated PLGA and 2D tissue culture plates. Our results demonstrated that the decellularized scaffolds promoted cell adhesion, proliferation, and osteogenic differentiation. Incorporating native components of bone-ECM with PLGA scaffolds has proven to be a successful approach to tissue engineering bone. A more detailed study is warranted to parse the *in vivo* mechanisms by which ECM proteins regulate osteogenesis.

Acknowledgments

We gratefully acknowledge support from the National Institutes of Health (Grant NIH P20 GM103641) and National Science Foundation (Grant EPS-0903795).

Disclosure Statement

No competing financial interests exist.

References

1. Giannoudis, P.V., Dinopoulos, H., and Tsiridis, E. Bone substitutes: an update. Injury **36 Suppl 3,** S20, 2005.
2. Parikh, S.N. Bone graft substitutes in modern orthopedics. Orthopedics **25,** 1301; quiz 1310; 2002.
3. Laurencin, C.T., Ambrosio, A.M., Borden, M.D., and Cooper, J.A., Jr. Tissue engineering: orthopedic applications. Annu Rev Biomed Eng **1,** 19, 1999.
4. Biermann, J.S., Holt, G.E., Lewis, V.O., Schwartz, H.S., and Yaszemski, M.J. Metastatic bone disease: diagnosis, evaluation, and treatment. J Bone Joint Surg Am **91,** 1518, 2009.
5. Muscolo, D.L., Ayerza, M.A., Aponte-Tinao, L.A., and Ranalletta, M. Use of distal femoral osteoarticular allografts in limb salvage surgery. Surgical technique. J Bone Joint Surg Am **88 Suppl 1 Pt 2,** 305, 2006.
6. Johari, A., Shingade, V., Gajiwala, A.L., Shah, V., and D'Lima, C. The use of irradiated allograft in a paediatric population: an Indian experience. Cell Tissue Bank **8,** 13, 2007.
7. Buck, B.E., Malinin, T.I., and Brown, M.D. Bone transplantation and human immunodeficiency virus. An estimate of risk of acquired immunodeficiency syndrome (AIDS). Clin Orthop Relat Res 129, 1989.
8. Lewandrowski, K.U., Rebmann, V., Passler, M., Schollmeier, G., Ekkernkamp, A., Grosse-Wilde, H., *et al.* Immune response to perforated and partially demineralized bone allografts. J Orthop Sci **6,** 545, 2001.
9. Moreau, M.F., Gallois, Y., Basle, M.F., and Chappard, D. Gamma irradiation of human bone allografts alters medullary lipids and releases toxic compounds for osteoblast-like cells. Biomaterials **21,** 369, 2000.
10. Mankin, H.J., Hornicek, F.J., and Raskin, K.A. Infection in massive bone allografts. Clin Orthop Relat Res 210, 2005.
11. Kessler, P., Thorwarth, M., Bloch-Birkholz, A., Nkenke, E., and Neukam, F.W. Harvesting of bone from the iliac crest—comparison of the anterior and posterior sites. Br J Oral Maxillofac Surg **43,** 51, 2005.
12. Salgado, A.J., Coutinho, O.P., and Reis, R.L. Bone tissue engineering: state of the art and future trends. Macromol Biosci **4,** 743, 2004.
13. Langer, R., and Tirrell, D.A. Designing materials for biology and medicine. Nature **428,** 487, 2004.

14. Jadlowiec, J.A., Celil, A.B., and Hollinger, J.O. Bone tissue engineering: recent advances and promising therapeutic agents. Expert Opin Biol Ther **3,** 409, 2003.
15. Murphy, W.L., and Mooney, D.J. Molecular-scale biomimicry. Nat Biotechnol **20,** 30, 2002.
16. Langer, R., and Vacanti, J.P. Tissue engineering. Science **260,** 920, 1993.
17. Karageorgiou, V., and Kaplan, D. Porosity of 3D biomaterial scaffolds and osteogenesis. Biomaterials **26,** 5474, 2005.
18. Hollister, S.J., Maddox, R.D., and Taboas, J.M. Optimal design and fabrication of scaffolds to mimic tissue properties and satisfy biological constraints. Biomaterials **23,** 4095, 2002.
19. Hollister, S.J., and Murphy, W.L. Scaffold translation: barriers between concept and clinic. Tissue Eng Part B Rev **17,** 459, 2011.
20. Khan, Y., Yaszemski, M.J., Mikos, A.G., and Laurencin, C.T. Tissue engineering of bone: material and matrix considerations. J Bone Joint Surg Am **90 Suppl 1,** 36, 2008.
21. Mikos, A.G., Herring, S.W., Ochareon, P., Elisseeff, J., Lu, H.H., Kandel, R., *et al.* Engineering complex tissues. Tissue Eng **12,** 3307, 2006.
22. Balasundaram, G., and Webster, T.J. Nanotechnology and biomaterials for orthopedic medical applications. Nanomedicine (Lond) **1,** 169, 2006.
23. Athanasiou, K.A., Agrawal, C.M., Barber, F.A., and Burkhart, S.S. Orthopaedic applications for PLA-PGA biodegradable polymers. Arthroscopy **14,** 726, 1998.
24. Mano, J.F., Sousa, R.A., Boesel, L.F., Neves, N.M., and Reis, R.L. Bloinert, biodegradable and injectable polymeric matrix composites for hard tissue replacement: state of the art and recent developments. Compos Sci Technol **64,** 789, 2004.
25. Mooney, D.J., Baldwin, D.F., Suh, N.P., Vacanti, J.P., and Langer, R. Novel approach to fabricate porous sponges of poly(D,L-lactic-co-glycolic acid) without the use of organic solvents. Biomaterials **17,** 1417, 1996.
26. Borden, M., Attawia, M., and Laurencin, C.T. The sintered microsphere matrix for bone tissue engineering: *in vitro* osteoconductivity studies. J Biomed Mater Res **61,** 421, 2002.
27. Ma, P.X., and Choi, J.W. Biodegradable polymer scaffolds with well-defined interconnected spherical pore network. Tissue Eng **7,** 23, 2001.
28. Heng, B.C., Cao, T., Stanton, L.W., Robson, P., and Olsen, B. Strategies for directing the differentiation of stem cells into the osteogenic lineage *in vitro*. J Bone Miner Res **19,** 1379, 2004.
29. Kwan, M.D., Slater, B.J., Wan, D.C., and Longaker, M.T. Cell-based therapies for skeletal regenerative medicine. Hum Mol Genet **17,** R93, 2008.
30. Menendez, P., Bueno, C., and Wang, L. Human embryonic stem cells: a journey beyond cell replacement therapies. Cytotherapy **8,** 530, 2006.
31. Evans, M.J., and Kaufman, M.H. Establishment in culture of pluripotential cells from mouse embryos. Nature **292,** 154, 1981.
32. Martin, G.R. Isolation of a pluripotent cell line from early mouse embryos cultured in medium conditioned by teratocarcinoma stem cells. Proc Natl Acad Sci U S A **78,** 7634, 1981.
33. Thomson, J.A., Itskovitz-Eldor, J., Shapiro, S.S., Waknitz, M.A., Swiergiel, J.J., Marshall, V.S., *et al.* Embryonic stem cell lines derived from human blastocysts. Science **282,** 1145, 1998.
34. Itskovitz-Eldor, J., Schuldiner, M., Karsenti, D., Eden, A., Yanuka, O., Amit, M., *et al.* Differentiation of human embryonic stem cells into embryoid bodies compromising the three embryonic germ layers. Mol Med **6,** 88, 2000.
35. Dang, S.M., Kyba, M., Perlingeiro, R., Daley, G.Q., and Zandstra, P.W. Efficiency of embryoid body formation and hematopoietic development from embryonic stem cells in different culture systems. Biotechnol Bioeng **78,** 442, 2002.
36. Petite, H., Viateau, V., Bensaid, W., Meunier, A., de Pollak, C., Bourguignon, M., *et al.* Tissue-engineered bone regeneration. Nat Biotechnol **18,** 959, 2000.
37. Li, C., Vepari, C., Jin, H.J., Kim, H.J., and Kaplan, D.L. Electrospun silk-BMP-2 scaffolds for bone tissue engineering. Biomaterials **27,** 3115, 2006.
38. Bruder, S.P., Jaiswal, N., and Haynesworth, S.E. Growth kinetics, self-renewal, and the osteogenic potential of purified human mesenchymal stem cells during extensive subcultivation and following cryopreservation. J Cell Biochem **64,** 278, 1997.
39. Meinel, L., Karageorgiou, V., Fajardo, R., Snyder, B., Shinde-Patil, V., Zichner, L., *et al.* Bone tissue engineering using human mesenchymal stem cells: effects of scaffold material and medium flow. Ann Biomed Eng **32,** 112, 2004.
40. Haynesworth, S.E., Goshima, J., Goldberg, V.M., and Caplan, A.I. Characterization of cells with osteogenic potential from human marrow. Bone **13,** 81, 1992.
41. Jaiswal, N., Haynesworth, S.E., Caplan, A.I., and Bruder, S.P. Osteogenic differentiation of purified, culture-expanded human mesenchymal stem cells *in vitro*. J Cell Biochem **64,** 295, 1997.
42. Verfaillie, C.M. Adult stem cells: assessing the case for pluripotency. Trends Cell Biol **12,** 502, 2002.
43. Quarto, R., Thomas, D., and Liang, C.T. Bone progenitor-cell deficits and the age-associated decline in bone repair capacity. Calcif Tissue Int **56,** 123, 1995.
44. Meijer, G.J., de Bruijn, J.D., Koole, R., and van Blitterswijk, C.A. Cell-based bone tissue engineering. PLoS Med **4,** e9, 2007.
45. Cuomo, A.V., Virk, M., Petrigliano, F., Morgan, E.F., and Lieberman, J.R. Mesenchymal stem cell concentration and bone repair: potential pitfalls from bench to bedside. J Bone Joint Surg Am **91,** 1073, 2009.
46. Gage, F.H. Mammalian neural stem cells. Science **287,** 1433, 2000.
47. Lee, R.H., Kim, B., Choi, I., Kim, H., Choi, H.S., Suh, K., *et al.* Characterization and expression analysis of mesenchymal stem cells from human bone marrow and adipose tissue. Cell Physiol Biochem **14,** 311, 2004.
48. Zaidi, M. Skeletal remodeling in health and disease. Nat Med **13,** 791, 2007.
49. Karp, J.M., Ferreira, L.S., Khademhosseini, A., Kwon, A.H., Yeh, J., and Langer, R.S. Cultivation of human embryonic stem cells without the embryoid body step enhances osteogenesis *in vitro*. Stem Cells **24,** 835, 2006.
50. Ahn, S.E., Kim, S., Park, K.H., Moon, S.H., Lee, H.J., Kim, G.J., *et al.* Primary bone-derived cells induce osteogenic differentiation without exogenous factors in human embryonic stem cells. Biochem Biophys Res Commun **340,** 403, 2006.
51. Kuznetsov, S.A., Cherman, N., and Robey, P.G. *In vivo* bone formation by progeny of human embryonic stem cells. Stem Cells Dev **20,** 269, 2011.
52. Mateizel, I., De Becker, A., Van de Velde, H., De Rycke, M., Van Steirteghem, A., Cornelissen, R., *et al.* Efficient

differentiation of human embryonic stem cells into a homogeneous population of osteoprogenitor-like cells. Reprod Biomed Online **16,** 741, 2008.
53. James, D., Nam, H.S., Seandel, M., Nolan, D., Janovitz, T., Tomishima, M., *et al.* Expansion and maintenance of human embryonic stem cell-derived endothelial cells by TGFbeta inhibition is Id1 dependent. Nat Biotechnol **28,** 161, 2010.
54. Lee, H., Shamy, G.A., Elkabetz, Y., Schofield, C.M., Harrsion, N.L., Panagiotakos, G., *et al.* Directed differentiation and transplantation of human embryonic stem cell-derived motoneurons. Stem Cells **25,** 1931, 2007.
55. Datta, N., Holtorf, H.L., Sikavitsas, V.I., Jansen, J.A., and Mikos, A.G. Effect of bone extracellular matrix synthesized *in vitro* on the osteoblastic differentiation of marrow stromal cells. Biomaterials **26,** 971, 2005.
56. Marcos-Campos, I., Marolt, D., Petridis, P., Bhumiratana, S., Schmidt, D., and Vunjak-Novakovic, G. Bone scaffold architecture modulates the development of mineralized bone matrix by human embryonic stem cells. Biomaterials **33,** 8329, 2012.
57. Peel, S.A., Hu, Z.M., and Clokie, C.M. In search of the ideal bone morphogenetic protein delivery system: *in vitro* studies on demineralized bone matrix, purified, and recombinant bone morphogenetic protein. J Craniofac Surg **14,** 284, 2003.
58. Zambonin, G., and Grano, M. Biomaterials in orthopaedic surgery: effects of different hydroxyapatites and demineralized bone matrix on proliferation rate and bone matrix synthesis by human osteoblasts. Biomaterials **16,** 397, 1995.
59. Hott, M., Noel, B., Bernache-Assolant, D., Rey, C., and Marie, P.J. Proliferation and differentiation of human trabecular osteoblastic cells on hydroxyapatite. J Biomed Mater Res **37,** 508, 1997.
60. Ong, J.L., Carnes, D.L., and Sogal, A. Effect of transforming growth factor-beta on osteoblast cells cultured on 3 different hydroxyapatite surfaces. Int J Oral Maxillofac Implants **14,** 217, 1999.
61. Toquet, J., Rohanizadeh, R., Guicheux, J., Couillaud, S., Passuti, N., Daculsi, G., *et al.* Osteogenic potential *in vitro* of human bone marrow cells cultured on macroporous biphasic calcium phosphate ceramic. J Biomed Mater Res **44,** 98, 1999.
62. Acil, Y., Terheyden, H., Dunsche, A., Fleiner, B., and Jepsen, S. Three-dimensional cultivation of human osteoblast-like cells on highly porous natural bone mineral. J Biomed Mater Res **51,** 703, 2000.
63. Knabe, C., Driessens, F.C., Planell, J.A., Gildenhaar, R., Berger, G., Reif, D., *et al.* Evaluation of calcium phosphates and experimental calcium phosphate bone cements using osteogenic cultures. J Biomed Mater Res **52,** 498, 2000.
64. Ohgushi, H., Miyake, J., and Tateishi, T. Mesenchymal stem cells and bioceramics: strategies to regenerate the skeleton. Novartis Found Symp **249,** 118; discussion 127, 170, 239; 2003.
65. Pham, Q.P., Kasper, F.K., Scott Baggett, L., Raphael, R.M., Jansen, J.A., and Mikos, A.G. The influence of an *in vitro* generated bone-like extracellular matrix on osteoblastic gene expression of marrow stromal cells. Biomaterials **29,** 2729, 2008.
66. Rho, J.Y., Kuhn-Spearing, L., and Zioupos, P. Mechanical properties and the hierarchical structure of bone. Med Eng Phys **20,** 92, 1998.
67. Borden, M., El-Amin, S.F., Attawia, M., and Laurencin, C.T. Structural and human cellular assessment of a novel microsphere-based tissue engineered scaffold for bone repair. Biomaterials **24,** 597, 2003.
68. Jukes, J.M., Both, S.K., Leusink, A., Sterk, L.M.T., Van Blitterswijk, C.A., and De Boer, J. Endochondral bone tissue engineering using embryonic stem cells. Proc Natl Acad Sci U S A **105,** 6840, 2008.
69. Jiang, T., Abdel-Fattah, W.I., and Laurencin, C.T. *In vitro* evaluation of chitosan/poly(lactic acid-glycolic acid) sintered microsphere scaffolds for bone tissue engineering. Biomaterials **27,** 4894, 2006.
70. Boskey, A.L. Matrix proteins and mineralization: an overview. Connect Tissue Res **35,** 357, 1996.
71. Declercq, H.A., Verbeeck, R.M., De Ridder, L.I., Schacht, E.H., and Cornelissen, M.J. Calcification as an indicator of osteoinductive capacity of biomaterials in osteoblastic cell cultures. Biomaterials **26,** 4964, 2005.
72. Tremoleda, J.L., Forsyth, N.R., Khan, N.S., Wojtacha, D., Christodoulou, I., Tye, B.J., *et al.* Bone tissue formation from human embryonic stem cells *in vivo*. Cloning Stem Cells **10,** 119, 2008.
73. Jukes, J.M., Both, S.K., van Blitterswijk, C.A., and de Boer, J. Potential of embryonic stem cells for *in vivo* bone regeneration. Regen Med **3,** 783, 2008.
74. Trounson, A. Human embryonic stem cells: mother of all cell and tissue types. Reprod Biomed Online **4 Suppl 1,** 58, 2002.

Address correspondence to:
Ehsan Jabbarzadeh, PhD
Department of Chemical Engineering
University of South Carolina
Columbia, SC 29208

E-mail: jabbarza@cec.sc.edu

Received: July 11, 2013
Accepted: February 19, 2014
Online Publication Date: June 18, 2014